THE FUNCTIONAL MORPHOLOGY OF THE AVIAN FLIGHT MUSCLE M. CORACOBRACHIALIS POSTERIOR

J. D. WOOLLEY*

Department of Ecology and Evolutionary Biology, Brown University, Providence, RI 02912, USA

*Present address: 533 Parnassus Avenue, Box 0662, SF CA, 94143, USA (e-mail: Joshua_Woolley@hotmail.com)

Summary

The extensive range of movement of the avian glenohumeral joint makes functional interpretation of any muscle that crosses the joint difficult. Multiple functional roles for the M. coracobrachialis posterior (CBP), an architecturally complex muscle that lies deep to the M. pectoralis, have been assigned on the basis of its anatomical position. The mechanical properties, neuromotor pattern during flight and the biochemical properties of the CBP in pigeons (*Columba livia*) were studied by *in situ* length/active tension and length/passive tension measurements, *in vivo* electromyography and muscle histochemistry. The action of the muscle was studied directly through *in situ* stimulation and measurement of humeral excursion in non-reduced preparations.

Key words: length–force, coracobrachialis posterior, muscle, bird flight, flight evolution, flight muscle, flight control, pigeon, *Columba livia*.

Introduction

The evolution of powered flight in birds is associated with extensive modification of the shoulder apparatus from the ancestral theropod condition. Late Jurassic and Early Cretaceous fossils reveal the basic reorganization of the shoulder joint, which includes elongation of the coracoids, scapulae aligned with the vertebral column which join the coracoid at an acute angle, a furcula in at least two specimens, and the keeled sternum that is often considered critical for flight (Poore et al., 1997; for a review, see Chiappe, 1995). Much discussion of the origin of flight has focused on the sternal keel and the triosseal canal, two features related to the two main flight muscles, the M. pectoralis and the M. supracoracoideus. Another feature that has undergone a significant change in the evolution of flight is the internal tuberosity (ventral tuberosity) of the proximal humerus. In modern birds, the internal tuberosity is a well-developed caudal projection on the proximal humerus separated from the humeral head by the capital groove onto which the Mm. subcoracoideus, coracobrachialis posterior (CBP) and the subscapularis insert (Raikow, 1985). The first evidence of the M. coracobrachialis posterior inserting onto a derived caudally projecting internal tuberosity is found in the Enantiornithines, a group that shares many features correlated with flight seen in extant birds (Chiappe and Calvo, 1994).

The CBP is an anatomically complex, highly pinnate muscle, with two distinct heads, that lies deep to the M. pectoralis. The medial head of the CBP originates on the posterior two-thirds of the ventro-medial aspect of the coracoid and a small portion of the sternum. The lateral head originates from the lateral process of the coracoid. Both heads converge to a strong common tendon to insert on the robust internal tuberosity of the humerus. The action of the M. coracobrachialis posterior has variously been described as chiefly supinating the wing with a slight depressing action (Sy, 1936), helping 'to pull the humerus posteriorly, folding it against the body, possibly with a slight rotation' (Hudson and Lanzilotti, 1955), depressing the wing (Chamberlain, 1943), assisting the [M. supracoracoideus] in elevating the humerus (Shufeldt, 1890), adduction (Harvey et al., 1968), depressing and dorsally rotating the humerus (Raikow, 1985) and depressing and retracting the wing (Dial et al., 1991). The homology of this muscle is also unclear.

To clarify the role of the CBP and its significance in the evolution of powered flight in birds, the *in situ* contractile properties of the muscle, including active and passive length–force characteristics and maximal force production, were investigated. Its *in vivo* electrical activity pattern during free flight and its contribution to humeral excursion during *in situ* stimulation were also determined. In addition, the anatomy of the muscle and tendon was studied. The presence or absence of the modern architecture of the CBP in fossil forms was determined by interpretation of published reports on the osteological anatomy of fossil birds.

One strategy for joint stabilization is simultaneous contraction of antagonistic muscles. In the avian shoulder, the M. supracoracoideus is generally considered to be the antagonist to the main wing depressor, the M. pectoralis. However, the CBP also produces antagonistic movements to the M. pectoralis. Furthermore, evidence of a modern morphology of the internal tuberosity and a large-keeled

sternum, which indicates the presence of a robust M pectoralis, are both first seen in the Enantiornithines (Walker, 1981; Chiappe and Calvo, 1994; Sanz et al., 1988, 1995, 1996; Sanz and Buscalioni, 1992; Wellenhoffer, 1994). Thus, the modern CBP morphology may have co-evolved with a massive M. pectoralis to help control the shoulder joint of the modern avian wing.

Materials and methods

Experiments were performed on 11 wild-type pigeons (*Columba livia* L.) with a mean body mass of 365±35 g (mean ± S.D.). The *in situ* isometric force of the M. coracobrachialis posterior (CBP) and active and passive length–force relationships were determined for four anesthetized birds, and its electrical activity during free flight was monitored for three birds. Birds were administered ketamine (60 mg kg^{-1}) and xylazine (6 mg kg^{-1}) intramuscularly to induce deep anesthesia for all surgical procedures. Additional ketamine was administered as necessary. The histochemistry of the CPB was studied in three birds, and the extent of humeral rotation and elevation was examined in one bird. Two of the birds used in these experiments and two additional specimens were dissected to investigate the anatomy of the CBP. Birds were acquired locally and maintained in the Brown University Animal Care Facility. They were fed cracked corn and given water (*ad libitum*). This study was performed in accordance with NIH Guidelines on the Use of Animals in Research.

Non-reduced preparations

The extent of humeral rotation, retraction and depression were measured during direct muscle stimulation *in situ* in an intact adult pigeon (*N*=1). Following anesthesia, the feathers over the pectoralis and wing were removed, and bipolar stimulating electrodes (100 μm diameter, 1.0 cm exposure) were surgically inserted into the CBP. The bird was held stationary by a sternal clamp, and the wing was hand-held while the CBP was activated (0.2 ms pulse; 60–100 Hz, 2.0 s train duration), and the extent of humeral long-axis rotation, retraction and depression were measured using a hand-held protractor. Pre-stimulation wing positions were also measured using a hand-held protractor. Electrode placement was verified through muscle palpation during muscle stimulation and through dissection after the bird had been killed. This procedure will be referred to as non-reduced to distinguish it from the length–tension experiments.

Length–tension experiments

Acute *in situ* experiments on adult pigeons (*N*=4) were performed after surgical isolation of the CBP. The feathers were removed from the entire left shoulder, breast and brachium. A lateral incision in the abdominal region was made and, after the abdominal air sacs had been opened, a tracheal tube was inserted to provide unidirectional ventilation of warmed and humidified oxygen (100 %). Care was taken not to interrupt the blood supply to the muscle, and body temperature was maintained at 39 °C with warmed avian Ringer and/or a heat lamp. Deflection and amputation of the M. pectoralis exposed the muscle. With the exception of the nerve to the CBP, all nerves in the brachial plexus were severed to avoid their activation through reflex action or volume conduction. Bipolar electrodes (custom-made, bipolar stainless-steel hooks with 1 mm exposure and 1–2 mm inter-tip distance) in contact with the exposed nerve were used to stimulate the muscle. Fine wire bipolar electrodes (insulated silver, 100 μm diameter, 0.5 mm tip exposure, 1 mm inter-tip distance) were inserted into the CBP with the aid of a 25 gauge needle to allow for monitoring of electromyographic signals. The muscles that run from the acromium of the scapula and the acrocoracoid process to the humerus (Mm. deltoideus complex and propatagialis complex) were transected and reflected, as were the muscles adjacent to the CBP, which insert onto the internal tuberosity of the humerus (Mm. scapulohumeralis caudalis and subcoracoideus). The tendon of the M. supracoracoideus was also transected.

The bird was mounted onto a heavy frame by clamping the carina of the sternum, the acrocoracoid process of the coracoid and the medial border of the scapula. The humerus was positioned to a known reference angle, and the length of the CBP was measured. A reference marker was tied around the tendon for later correlation of whole muscle length (from the reference marker to the lateral process of the coracoid) to humeral joint angles *in vivo*. This tie was used to measure the length of the CBP throughout the experiment. Subsequently, the bone surrounding the point of attachment of the CBP's tendon was cut using a dremmel tool, and this bone/tendon structure was attached to a force transducer by a short piece of silk (compliance 0.45 μm N^{-1} cm^{-1}). The force transducer was mounted on an adjustable rack and pinion (millimeter calibration) along the longitudinal axis of the CBP, which allowed incremental muscle length change.

The passive and active length–force properties of the muscle at a series of lengths encompassing its normal *in vivo* excursion were measured. Measurements were made starting at lengths at which the muscle was almost completely slack and ending when it was unnaturally tense. This guaranteed that the *in vivo* lengths were included in the sample. The active length–force curve was generated from maximal tetanic responses (0.2 ms pulse duration, 60 Hz, 500 ms train duration). Each curve was generated by lengthening the muscle in 1.0 mm increments over its physiological working range. Between each measurement, the muscle was returned to the length for 'zero' passive tension, 5.0 s was allowed to elapse, and the muscle was then pulled to a new longer length. All data were digitally recorded (10 MHz) and stored on disk for off-line analysis on a Nicolet 400 series waveform acquisition system.

The absolute muscle length was correlated with humeral position by manipulating the contralateral wing in each bird after it had been killed (sodium pentobarbital, 100 mg kg^{-1}). The CBP was isolated, the bird was mounted in a stereotaxic frame, and the humerus was positioned at the reference angle. A new string was tied around the intact CBP, and the humerus

was positioned at various degrees of depression/elevation and pronation/supination while the length of the CBP was simultaneously measured. In this way, *in situ* force measurements could be correlated to actual humeral positions. In addition, the approximate minimum and maximum *in vivo* muscle lengths were estimated by positioning the humerus at *in vivo* joint angles estimated from Brown (1951) and Simpson (1983) and from sequences of pigeons in flight recorded for electromyographic analysis while simultaneously measuring the length of the CBP.

Muscle histochemistry

When the bird had been killed, the CBP muscle (N=3) was removed in its entirety for histochemical analysis. The muscle was cut into 3–5 blocks of $10\,cm^2$. Care was taken to preserve the fiber orientation. Blocks were frozen in isopentane at $-160\,^{\circ}C$ and stored at $-70\,^{\circ}C$. Cryostat cross sections of $12\,\mu m$ thickness were cut in groups of three serial sections throughout the length of the muscle at $-20\,^{\circ}C$ and mounted directly onto coverslips. These sections were reacted for reduced nicotinamide adenine dinucleotide diaphorase (NADH-D) to determine muscle fiber oxidative capacity, for α-glycerophosphate dehydrogenase (α-GPD) to determine glycolytic activity and for myofibrillar adenosine triphosphatase (ATPase) to determine whether muscle fibers were 'fast' or 'slow' (Kaplan and Goslow, 1989). Serial staining of NADH-D, α-GPD and ATPase allowed multiple properties of the same muscle cell to be determined. The cross-sectional areas of these muscle fibers were calculated from the NADH-D sections because these boundaries were most clearly defined. The cross-sectional areas of 647 muscle fibers from within the medial head and 402 fibers from within the lateral head were determined. Sections were viewed under a microscope, and digital (eight-bit gray-scale) images of each section were acquired at $200\times$ magnification using a CCD camera and analyzed using NIH Image software (W. Rasband, National Institutes of Health) and a Macintosh computer.

Electromyography

The electrical activity pattern of the CBP was determined through *in vivo* electromyography (EMG) of free-flying pigeons (N=3). The flights were simultaneously filmed using high-speed video ($1000\,images\,s^{-1}$; Kineview System, manufactured by Adaptive Optics Associates Inc.) synchronized with the EMG. All data were recorded digitally ($10\,MHz$) and stored on disk for off-line analysis on a Nicolet 400 series waveform acquisition system. Pigeons were trained to fly in a brightly lit hallway and to land on their cage (waist level). The birds were trained to carry a weight on their back to simulate the multi-pin connector used during recording. The camera was positioned at slightly above waist level $3.7\,m$ perpendicular to the flight path. At the onset of the surgical procedure, the pigeon was anesthetized ($60\,mg\,kg^{-1}$ ketamine and $6\,mg\,kg^{-1}$ xylazene), and a longitudinal incision was made through the skin just lateral to the scapula to expose the dorsal aspect of the M. pectoralis (thoracobrachialis) and the M.

scapulohumeralis caudalis. Separation of these muscles revealed the CBP. A longitudinal incision was made along the dorsal midline from the caudal ends of the scapulae to the synsacrum, and a custom-made multi-pin plug was sutured to the fascia surrounding the spine. The EMG wires (insulated silver, $100\,\mu m$ diameter, $0.5\,mm$ tip exposure, $1\,mm$ inter-tip distance) were run subcutaneously to the previous incision and with a 25 gauge needle; one pair was inserted into the CBP and the second pair into the M. pectoralis. This allowed visual confirmation of electrode placement within the CBP. The incisions were sutured, and the bird was allowed to recover overnight with intermittent visual monitoring. The location of the electrodes was verified through back-stimulation with visual confirmation of muscle contraction and evidence of the appropriate movement caused by the muscle in all three birds prior to the initiation of recording. Electrode placement was verified by dissection in two birds after the final recording session after the birds had been killed.

Results

Anatomy

In *Columba livia*, the M. coracobrachialis posterior (CBP) consists of two distinct heads separated by a tendinous sheath (Figs 1, 2). The medial head arises from the lateral surface of the posterior two-thirds of the coracoid and a small portion of the sternum, while the lateral head originates by a tendon from the terminus of the coracoid, the lateral process. This separation is supported by the histochemical results, which show two distinct histochemical portions that coincide with the two heads even though they are innervated by a single nerve. The two heads run together to form a strong flat tendon that inserts onto the capital groove of the internal tuberosity (Fig. 2). This position causes the tendon to course up and over the internal tuberosity to insert on its dorsal aspect when the wing is horizontal. The tendon has a cup-like pit that fits snuggly over the internal tuberosity when the humerus is pronated. This tendinous cup does not disappear if the tendon is pulled taut with forceps.
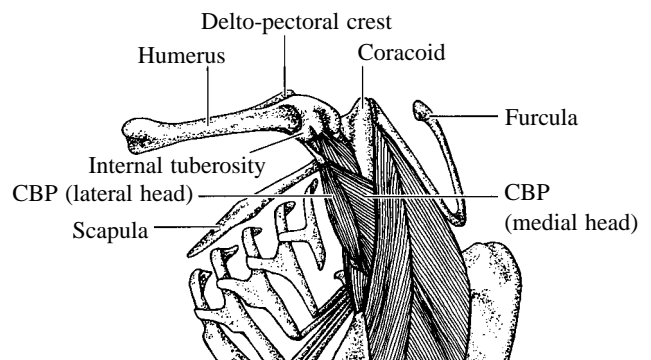

Fig. 1. Ventro-lateral view of the deep musculature of the shoulder in the pigeon (*Columba livia*) with the humerus rotated dorsally. The two heads of the M. coracobrachialis posterior (CBP) insert by a strong common tendon onto the internal tuberosity of the humerus.
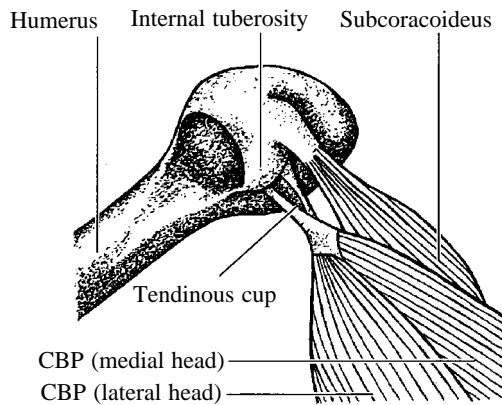
Fig. 2. Ventro-lateral view of the insertion of the M. coracobrachialis posterior (CBP) in the pigeon (*Columba livia*). The internal tuberosity fits snuggly on the tendon of the CBP.

Humeral excursion

The movement of the humeral head through and within the glenoid is extremely complex. As the humerus moves through the downstroke during flight, there is both adduction and simultaneous rotation about its longitudinal axis. While the extremes of rotation are limited by the coracohumeral (pronation) and scapulohumeral (supination) ligaments (Sy, 1936; Jenkins, 1993), the humerus has extensive freedom of movement between these two extremes, making its kinematics difficult to describe (Sy, 1936; Simpson, 1983). As a result, humeral position is reported as instantaneous angles of elevation and rotation. In this report, 0° elevation and pronation correspond to a wing position where the wing is in the horizontal plane with no long-axis rotation. As the wing is raised and supinated, the angle of elevation increases and the angle of pronation decreases. Protraction of 0° refers to the position in which the humerus is parallel with the vertebral column in the horizontal plane. As the humerus moves away from the body in this plane, the angle of protraction increases.

Non-reduced preparation

At a wing position appropriate for the beginning of downstroke (approximately 53° elevation, approximately −1° protraction), CBP stimulation induced the angle between the humerus and the vertebral column to decrease (by approximately 10°) in addition to producing slight supination. Stimulation of the CBP at the wing position where the humerus passes the horizontal (elevation approximately 0°, protraction approximately 70° and pronation approximately 0°), induced substantial supination (approximately 18–20°) with little or no retraction. When the angle of protraction was greater than approximately 70°, a small retractive component was seen. CBP stimulation at the wing position appropriate for the bottom of the downstroke (approximately −32° elevation, approximately 55° protraction and approximately 38° pronation), induced supination (approximately 20°) with no retraction. When the angle of protraction was increased beyond
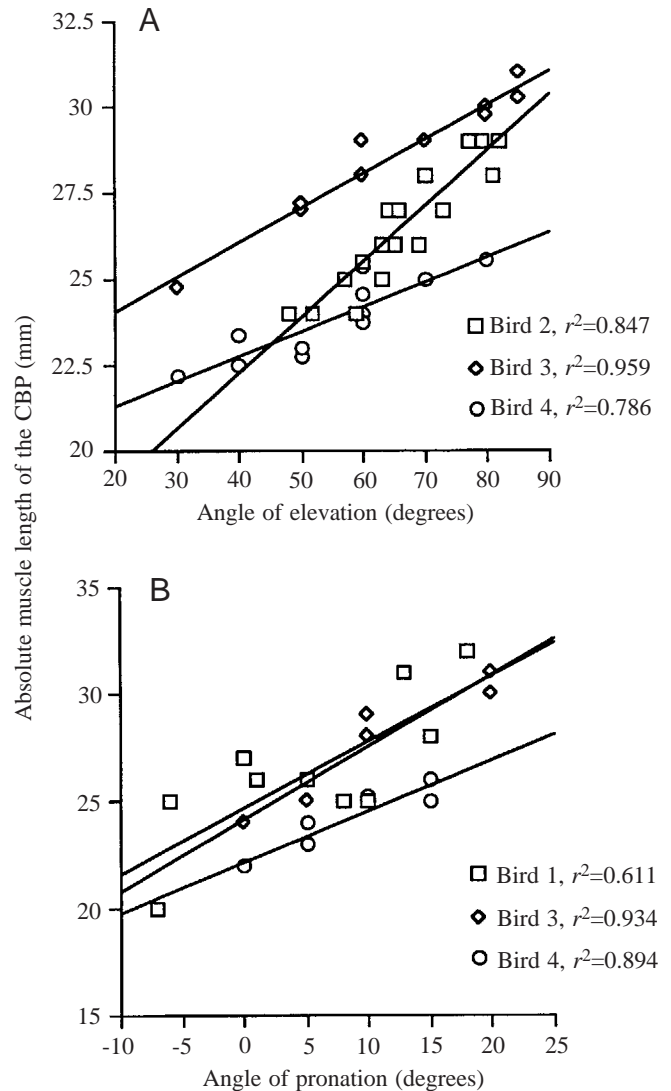

Fig. 3. Absolute muscle measurements of the M. coracobrachialis posterior (CBP) from the lateral process of the coracoid to the end of the muscular fibers plotted against (A) the angle between the humerus and the spine at the beginning of the downstroke (angle of elevation) and (B) long-axis rotation of the humerus at mid-downstroke (angle of pronation). These measurements were used in conjunction with force–length measurements to generate 2 force–angle curves (see Fig. 5). Different symbols identify different birds. Least-squares regression lines are shown for each bird where significant ($P<0.05$ for all).

approximately 55° and the CBP stimulated, a retractive component was observed.

Length–tension experiments

The CBP generates peak tetanic forces of three times the bird's weight (8.5±0.3 N, mean ± S.E.M., $N=3$) and has a steep passive-tension curve. The relationship between muscle length and wing excursion is difficult to quantify because of the universal nature of the glenohumeral joint. To simplify the problem, muscle length change was measured while a single positional variable was changed. Fig. 3 illustrates changes in
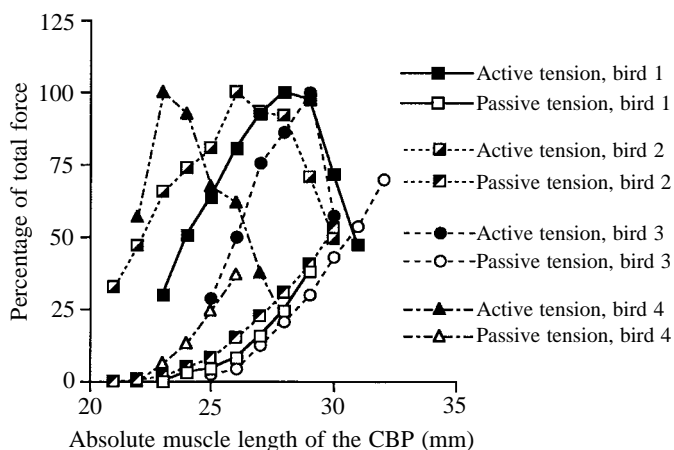
Fig. 4. Total isometric length–force curves of the M. coracobrachialis posterior (CBP) as function of absolute muscle length measured from the lateral process of the coracoid to the end of the muscular fibers. Active length–force curves were generated by eliciting tetanic responses (0.2 ms duration, 60 Hz, 500 ms train duration) at a series of lengths encompassing the normal excursion range of the muscle.

raw absolute muscle length in terms of wing position. Fig. 4 illustrates length–force curves in terms of raw absolute muscle lengths. These data sets were used in combination to create force–length curves in terms of angular positions of the humerus (Fig. 5). While the absolute length–angle relationships (Fig. 3) and the force–absolute length relationships (Fig. 4) are variable in different birds, when combined to give the force–angle relationship, the resultant curves (Fig. 5) are relatively consistent. It is important to note that, as muscle length increases, the ascending limb of the active length–tension curve corresponds to pronation of the humerus around the horizontal.

For bird 4, absolute active forces were approximately half those found in the other birds, while absolute values of passive forces were comparable. The cause of this discrepancy is unknown. The length–force relationship for this bird, however, was similar to those of the other birds, and these data were therefore included in the analysis. Since the passive forces for this bird represented an abnormally large proportion of total force, mean total forces from the other three experiments were used to calculate the percentage of total force (Figs 4, 5) for the passive curve of bird 4.

Histochemistry

Two distinct fiber-type compartments were discovered in the CBP that correspond to the lateral and medial heads (Fig. 6; Table 1). All fibers produce a dark reaction after alkaline preincubation, indicating ATPase stability (i.e. a 'fast' profile). Within the medial head, two distinct fiber-type cell populations were determined. These cells could be separated into two groups related to size (mean ± 95 % confidence interval) and reaction with NADH-D: (i) those with a mean cross-sectional area of $758\pm23\,\mu m^2$ and a dark reaction with NADH-D, and (ii) those with a mean cross-sectional area of $1712\pm49\,\mu m^2$ and
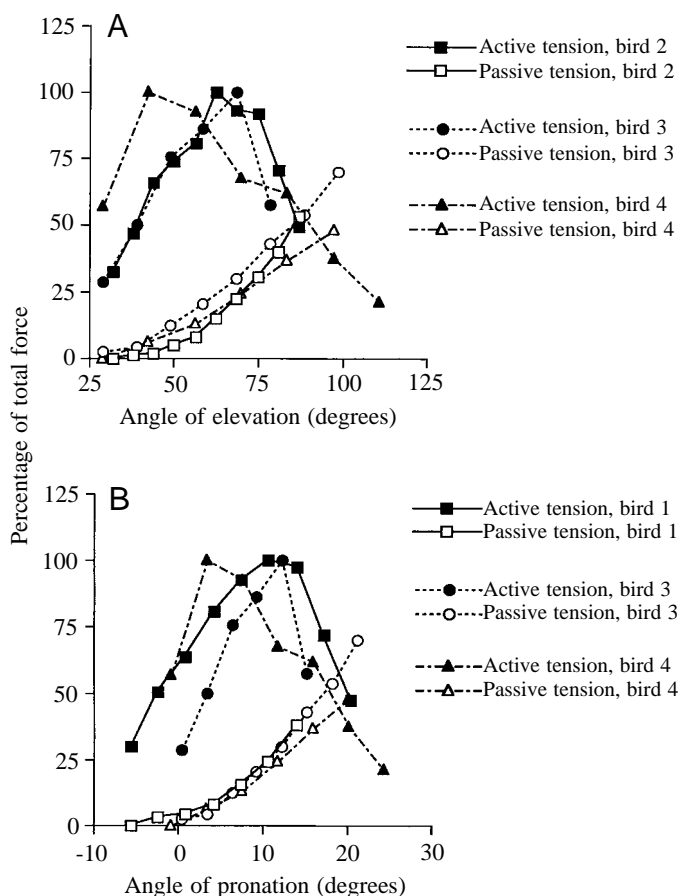

Fig. 5. Total isometric force–angle curves of the M. coracobrachialis posterior (CBP) in which length is plotted as a function of (A) elevation and (B) long-axis rotation. At the top of the downstroke, as the angle between the humerus and the spine increases, the potential for force increases (A). During the downstroke, as the pitch of the wing increases, the potential for force increases (B). *In vivo*, the muscle functions on the ascending limb of the active length–force curve at both humeral positions. Angles were derived from absolute muscle length as described in Materials and methods (see also Fig. 3).

a light reaction with NADH-D (Kaplan and Goslow, 1989). These two types have been assigned various names (Rosser and George, 1986). Here, the small fast oxidative-glycolytic cells are referred to as FOG and the large, fast non-oxidative glycolytic cells are referred to as FG. The FG fibers were predominantly found on the fascicular boundary, whereas the FOG fibers were predominately located centrally within the fasicle. This histochemical pattern is similar to that of the pectoralis in pigeons (Sokoloff et al., 1998). The lateral head consists of a homogeneous population of cells with a mean cross-sectional area of $864\pm23\,\mu m^2$ and a moderate reaction with NADH-D; i.e. FOG cells (Fig. 6; Table 1).

Electromyography

The CBP consistently exhibited electrical activity 7.9 ms, or 6.9±0.9 % (mean ± 95 % confidence interval) of a normalized wingbeat cycle, before the beginning of the downstroke and
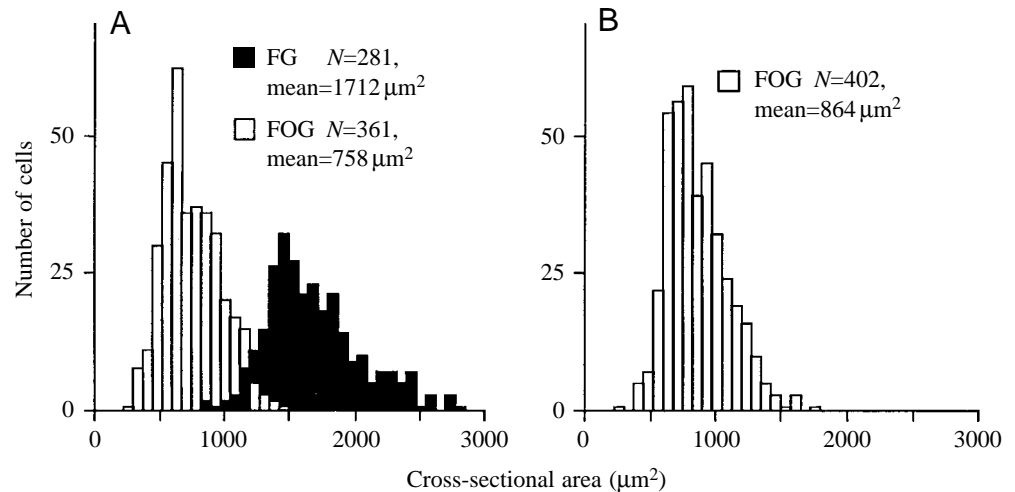
Fig. 6. Histograms illustrating cross-sectional areas of cells within the M. coracobrachialis posterior (CBP); (A) medial head; (B) lateral head. FG, fast glycolytic; FOG, fast oxidative glycolytic.

after the onset of the thoracobrachialis portion of the M. pectoralis (Fig. 7). The activity of the muscle ceased directly after the initiation of the upstroke and 34.4 ms, or 29.1 ± 1.4 % % of a normalized wingbeat cycle, after the thoracobrachialis portion of the M. pectoralis.

Discussion

In this study, a variety of complementary *in vivo* and *in situ* experimental techniques were used to explore the function of the CBP. Other studies of the relationship between contractile properties and muscle length have concentrated on the relationship between the architecture of a muscle and its length–tension properties (for a review, see Ettema and Huijing, 1994) or with the properties of individual sarcomeres (Gorden et al., 1966a,b; Keurs et al., 1978; Rack and Westbury, 1969). The present report is concerned with the more general issue of the function and evolution of a musculoskeletal system to meet the demands of flight.

Wing kinematics for the pigeon were estimated from Brown (1951) and Simpson (1983) and from sequences of pigeons in flight recorded for EMG analysis. The downstroke begins, in lateral view, with the humerus directly vertical from the shoulder at an angle of 53 ° with the vertebral column. As the

Table 1. *Cross-sectional area of cells from the coracobrachialis posterior muscle*

	Cross-sectional area of medial head (μm²)		Cross-sectional area of lateral head (μm²)
	FG	FOG	FOG
Mean	1712	758	864
S.E.M.	25	12	12
N	286	361	402
95 % confidence interval	±49	±23	±23

FG, fast glycolytic; FOG, fast oxidative glycolytic.

wing is depressed and the downstroke proceeds, there is significant protraction and pronation of the humerus. The humerus begins to be retracted before the end of the downstroke, and supination begins as the wing begins to elevate.

Functional implications of the length–tension properties of the CBP

Active and passive tension

As a pinnate muscle, the CBP is well designed for relatively high force production but is poorly suited to large excursion. The CBP produces peak tetanic forces of approximately 9 N or three times the bird's body weight. Since the length–tension curve of the CBPs is narrow, potential force rises quickly as length increases. In addition, unlike the supracoracoideus of pigeons, in which passive force is a relatively small component of total force (Poore et al., 1997), the CBP exhibits significant passive tension. The passive force in the CBP rises more quickly as length increases and is a larger component of total force at all lengths than in the supracoracoideus (30 % of peak tetanic force in the CBP compared with 7.6 % in the supracoracoideus; Poore et al., 1997) (Figs 4, 5). This arrangement of high potential force production over a short excursion with high passive tension is suitable for a wing-stabilizer or muscular strut.

At both wing positions examined, when the humerus is at the top of the downstroke (Fig. 5A) and when it passes through the horizontal plane (Fig. 5B), the CBP works along the ascending limb of its active length–tension curve. At the beginning of the downstroke (Fig. 5A), as the humerus is depressed, the CBP shortens along the ascending limb of its active length–tension curve. In the horizontal position (Fig. 5B), because of the pronation of the humerus, the CBP is lengthened along its ascending limb. A working range restricted to the ascending limb of the length–tension curve is consistent with reports of many, but not all, locomotor muscles (for a review, see Poore et al., 1997). The fact that the ascending limb of the length–tension curve of the CBP is correlated with pronation of the humerus supports the
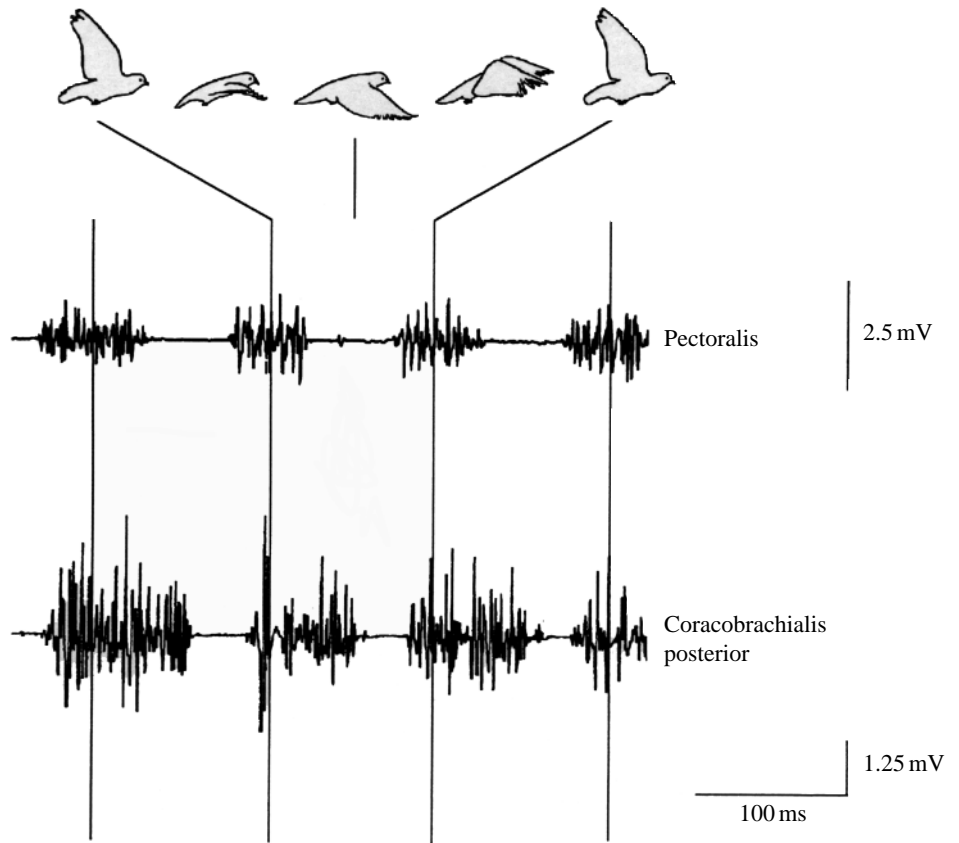
Fig. 7. Representative simultaneous electromyographic recordings from the flight muscles of a pigeon in free flight. Vertical lines represent the beginning of downstroke. The outlines above the recordings indicate the wing positions during the stroke.

hypothesis that it is important for the prevention of hyper-rotation during the downstroke.

Endo- and exosarcomeric lattices are thought to create and mediate muscle stiffness and viscoelasticity (Wang et al., 1993). Within the endosarcomeric lattice, elastic titin filaments have been shown to have similar stress–strain curves to those of the intact sarcomere. Differences in the distribution of titin isoforms directly alter the passive tension characteristics of a muscle: those that express larger titin isoforms initiate tension and reach their elastic limit at relatively longer lengths (Wang et al., 1991). In cardiac muscle, which exhibits stiff passive tension (e.g. Sonnenblick, 1962; Spiro and Sonnenblick, 1964), passive forces are thought to confine the muscle to working on the ascending limb of the active length–tension curve (Allen et al., 1974). The role of the high passive force in the CBP may be similar, restricting the work done by the CBP to the ascending limb of the active length–tension curve. Since the muscle is connected to the skeletal system, this confinement also contributes to the stabilization of the wing during the downstroke by acting as a stiff brace to counter hyper-rotation. This high passive tension might also assist the supracoracoideus in the initiation of supination at the beginning of the upstroke.

Despite different absolute muscle length–angle relationships (Fig. 3A,B), and different absolute muscle length–force relationships (Fig. 4), muscle force–angle relationships (Fig. 5A,B) are relatively consistent. This may reflect a change

in serial sarcomere number in individual birds to maximize force production at appropriate wing positions. Studies on the effects of limb immobilization on fiber length indicate that serial sarcomere number is highly plastic (for a review, see Burkholder and Leiber, 1998). In as little as 2 weeks, serial sarcomere number changes such that maximal force and optimal sarcomere length are produced at the position of immobilization. While the exact cues for this change remain unknown, it is clear that muscles adapt their length to align their length–force characteristics appropriately with their *in vivo* activity and function.

Whole muscle function in flight

Neural activation of the CBP begins at the end of the upstroke and continues through the downstroke to the beginning of the subsequent upstroke. These electrically active periods are not precisely coincident with force production because of an electromechanical delay (Goslow and Dial, 1990). The delay in force onset following the electrical onset is relatively small (<8 ms) and, thus, by the upstroke/downstroke transition, the CBP produces significant force as the wing pronates because of the action of the M. pectoralis. Stimulation studies and gross anatomy indicate, however, that the muscle's primary action is to supinate the wing. It is therefore proposed that the CBP is coactivated with the M. pectoralis to act as a dynamic muscular strut controlling the passage of the wing.

The CBP shortens as the humerus is depressed, but it lengthens as the humerus pronates. Thus, relatively little length change of the CBP during the downstroke is predicted. If, during the downstroke, there is hyper-pronation, the CBP is lengthened and works at a length coincident with higher total forces (active and passive), thereby increasing force to help correct the imbalance. This reduces the need for active neuromodulation. If, however, the humerus is inadvertently hypo-pronated, the CBP is shifted to the left on its length–tension curve, and force production decreases. In this situation, when the supinational force of the CBP is low, force from the M. pectoralis will be sufficient to pronate the humerus into the appropriate position. Similarly, the CBP retracts the wing at angles of protraction greater than those found in a normal wingbeat. Thus, if a pertubation causes hyper-protraction, the force of the CBP tends to bring the humerus back into its appropriate position. Furthermore, if the angle of protraction is smaller than found in a normal wingbeat, the substantial protractive forces produced by the sternobrachialis portion of the M. pectoralis (Dial et al., 1988) will act to bring the wing into correct alignment. This system is dynamic because the nervous system can modulate the contraction duration and intensity of the CBP depending on the general demands of flight.

The contractile properties of the CBP are compatible with this hypothesis. It produces relatively large tetanic and passive forces for its size that are appropriate for a stabilizing muscle. The length–tension curve is also fairly compressed (a steep increase in force production with increased muscular length) compared with that of the M. supracoracoideus in the pigeon (Poore et al., 1997). Furthermore, the ascending limb is coincident, at mid-downstroke, with long-axis rotation of the humerus about the horizontal plane. This is appropriate for a muscle that acts to prevent hyper-rotation of the humerus at the horizontal position.

The maximal isometric forces measured in this study are suitable for comparative purposes and should be considered as potential forces, not real forces, used by naturally behaving birds in flight. While *in vivo* force and length measurements have not yet been made for the CBP in any bird species, some predictions can be made. If the length of the CBP remains relatively constant during flight, *in situ* isometric length–tension curves would illustrate the optimal *in vivo* length for maximal force production. A muscle that contracts isometrically produces high force and no work, whereas a muscle that actively lengthens produces even higher forces but negative work. A shortening contraction that maximizes the rate of work production or power, however, only produces one-third of maximal force (Hill, 1950). It has been proposed that an organism can minimize the cost of producing force during running by operating muscles isometrically while the elastic recoil of tendinous springs provides the work (Roberts et al., 1997). The M. gastrocnemius has been shown to act isometrically during walking in the turkey (Roberts et al., 1997) and during hopping in the wallaby (Biewener, 1998). These muscles are designed to produce force economically to

facilitate tendon stretch and strain energy recovery. Furthermore, the M. pectoralis of the starling (*Sturnus vulgaris*) exhibits stretch-active contractions during late upstroke that provide large decelerating forces that stop the wing and reverse its direction at the upstroke–downstroke transition (Goslow and Dial, 1990). Similar principles may apply to the CBP in pigeons. Isometric or stretch-active contractions in the CBP allow for high force production in a relatively small muscle at relatively low metabolic cost.

If the CBP is a muscular strut, it will be in a state of contraction before it is actively lengthened by the musculo-skeletal system. As it is lengthened, its length–tension and force–velocity characteristics could provide a mechanism for high-speed control of the wing during flight. This 'feedforward' mechanism has the advantage of requiring little neural modulation during the downstroke to maintain the correct pitch of the wing. Mechanical properties alone could compensate for disturbances in the wing's trajectory. These mechanical properties are intrinsic to the muscle and thus act more rapidly than segmental neural control mechanisms that have a time delay before force can be produced. A similar system has been found in certain hexapods. The death-head cockroach (*Blaberus discoidalis*) is able to traverse rough terrain at full speed with no change in gait or EMG pattern (Full et al., 1999). These observations suggest that mechanical properties alone produce stability. Also, using a computer model of the cockroach, Kubow and Full (1999a) show recovery from a range of perturbations because of the 'dynamic coupling of yaw and lateral forces without feedback control'. Alterations in one velocity component necessarily alter the others, which consequently provide 'mechanical feedback' by altering leg moment arms (Kubow and Full, 1999b).

Evolution of the M. coracobrachialis posterior

The presence or absence of the modern architecture of the internal tuberosity in fossil forms can shed light on both the evolutionary history and the derived function of the CBP. In modern birds, the internal tuberosity is a well-developed caudal projection on the humerus separated from the humeral head by the capital groove, the insertion surface for the Mm. subcoracoideus, coracobrachialis posterior and the subscapularis (Raikow, 1985). Chiappe (1996) concluded that the retention of a less well-developed internal tuberosity that projects caudomedially with no capital groove, such as that seen in *Archaeopteryx,* dromaeosaurids and other non-avian therapods, to be primitive. The analysis of Zhou (1995) reveals the internal tuberosity to be absent from *Archaeopteryx* and *Confuciusornis sanctus* (the second most primitive bird currently known).

The first modern caudally projecting internal tuberosity is found in the Enantiornithines, a group that shares many features correlated with flight also present in extant birds (Chiappe, 1996). Chiappe and Calvo (1994) noted these features to include a 'prominent sternal keel, strut-like coracoids with close sternal articulations, low interclavicular angle, coracoid and scapula meeting at a sharp angle, [and a]

well-developed wing with typical proportions'. The internal tuberosity appears to have been lost in the flightless hesperonithiforms and to be greatly modified in the flightless ratites (Chiappe, 1996). That the internal tuberosity first appears in the Enantiornithines with their advanced flight apparatus, but is lost or modified in flightless forms, implies that the modern morphology of a caudally projecting internal tuberosity is important for powered flight. In *Iberomesornis romerali* and *Patagopteryx deferrariisi*, the ingroup taxa, the condition of the internal tuberosity is uncertain, and Chiappe (1996) concludes that a caudally projecting internal tuberosity is a synapomorphy of the Enantiornithines, *Patagopteryx deferrariisi* and the Ornithurae.

The Enantiornthines show not only the first modern internal tuberosity but also the first large ossified keeled sternum (Walker, 1981; Chiappe and Calvo, 1994; Sanz et al., 1988, 1995, 1996; Sanz and Buscalioni, 1992; Wellenhoffer, 1994). This may indicate that an advanced CBP co-evolved with the sternal keel, a structure indicative of a robust pectoralis, lending support to the hypothesis that the CBP functions as an antagonist to the M. pectoralis.

References

Allen, D. G., Jewell, B. R. and Murray, J. W. (1974). The contribution of activation processes to the length–tension relation of cardiac muscle. *Nature* **248**, 606–607.

Biewener, A. A. (1998). Muscle function *in vivo*: a comparison of muscles used for elastic energy savings *versus* muscles used to generate mechanical power. *Am. Zool.* **38**, 703–717.

Brown, R. H. J. (1951). Flapping flight. *Ibis* **93**, 335–359.

Burkholder, T. J. and Leiber, R. L. (1998). Sarcomere number adaptation after retinaculum transection in adult mice. *J. Exp. Biol.* **201**, 309–316.

Chamberlain, F. W. (1943). *Atlas of the Avian Anatomy*. East Lansing: Michigan State University Press.

Chiappe, L. M. (1995). The first 85 million years of avian evolution. *Nature* **378**, 349–355.

Chiappe, L. M. (1996). Late Cretaceous birds of Southern America: anatomy and systematics of the Enantiornithines and *Patagopteryx deferrariisi*. *Muncher Geoweiss. Abh.* A **30**, s203–s244.

Chiappe, L. M. and Calvo, J. O. (1994). *Neuquenornis volans*, a new Late Cretaceous bird (Enantiornithines: avisuridae) from Patagonia, Argentina. *J. Vert. Paleontol.* **14**, 230–246.

Dial, K. P., Goslow, G. E., Jr, and Jenkins, F. A., Jr (1991). The functional anatomy of the shoulder in the European starling (*Sturnus vulgaris*). *J. Morph.* **207**, 327–344.

Dial, K. P., Kaplan, S. R., Goslow, G. E., Jr and Jenkins, F. A., Jr (1988). A functional analysis of the primary upstroke and downstroke muscles in the domestic pigeon (*Columba livia*) during flight. *J. Exp. Biol.* **134**, 1–16.

Ettema, G. J. C. and Huijing, P. A. (1994). Effects of destribution of fiber length on active length–force characteristics of rat gastrocnemius medialis. *Anat. Rec.* **239**, 414–420.

Full, R. J., Autumn, K., Chung, J. I. and Ahn, A. (1999). Rapid negotiation of rough terrain by the death-head cockroach. *Am. Zool.* **39**, 81.

Gorden, A. M., Huxley, A. F. and Julian, F. J. (1966a). Tension development in highly stretched vertebrate muscle fibres. *J. Physiol., Lond.* **184**, 143–169.

Gorden, A. M., Huxley, A. F. and Julian, F. J. (1966b). The variation in isometric tension with sarcomere length in vertebrate muscle fibres. *J. Physiol., Lond.* **184**, 170–192.

Goslow, G. E., Jr and Dial, K. P. (1990). Active stretch–shorten contractions of the M. pectoralis in the European starling (*Sturnus vulgaris*): Evidence from electromyography and contractile properties. *Neth. J. Zool.* **40**, 106–114.

Harvey, E. B., Kaiser, H. E. and Rosenberg, L. E. (1968). *An Atlas of the Domestic Turkey*. Washington DC: US Atomic Energy Commission.

Hill, A. V. (1950). The dimensions of animals and their muscular dynamics. *Sci. Prog.* **150**, 209–230.

Hudson, G. E. and Lanzilotti, P. J. (1955). Gross anatomy of the wing muscles in the family Corvidae. *Am. Midl. Nat.* **53**, 1–53.

Jenkins, F. A., Jr (1993). The evolution of the avian shoulder joint. *Am. J. Sci.* **293**A, 253–367.

Kaplan, S. R. and Goslow, G. E., Jr (1989). Neuromuscular organization of the pectoralis (pars thoracicus) of the pigeon (*Columba livia*): Implications for motor control. *Anat. Rec.* **224**, 426–430.

Keurs, H. E. D. J. T., Iwasumi, T. and Pollack, G. H. (1978). The sarcomere length–tension relation in skeletal muscle. *J. Gen. Physiol.* **72**, 565–592.

Kubow, T. M. and Full, R. J. (1999a). Effects of changing morphology on running stability shown by linearization of a two dimensional hexapod model. *Am. Zool.* **38**, 81A.

Kubow, T. M. and Full, R. J. (1999b). The role of the mechanical system in control: a hypothesis of self-stabilization in hexapedal runners. *Phil. Trans. R. Soc. Lond.* B **354**, 849–862.

Poore, S. O., Ashcroft, A., Sanchez-Haiman, A. and Goslow, G. E., Jr (1997). The contractile properties of the M. supracoracoideus in the pigeon and starling: a case for long-axis rotation of the humerus. *J. Exp. Biol.* **200**, 2987–3002.

Rack, P. M. H. and Westbury, D. R. (1969). The effects of length and stimulus rate on tension in the isometric cat soleus muscle. *J. Physiol., Lond.* **204**, 443–460.

Raikow, R. (1985). Locomotor systems. In *Form and Function in Birds*, vol. III (ed. A. S. King and J. McLelland), pp. 57–147. London: Academic Press.

Roberts, T. J., Marsh, R. L., Weyand, P. G. and Taylor, C. R. (1997). Muscular force in running turkeys: the economy of minimizing work. *Science* **275**, 1113–1115.

Rosser, B. W. C. and George, J. C. (1986). The avian pectoralis: histochemical characterization and distribution of muscle fiber types. *Can. J. Zool.* **64**, 1174–1185.

Sanz, J. L., Bonaparte, J. F. and Lacasa, A. (1988). Unusual Early Cretaceous birds from Spain. *Nature* **331**, 433–435.

Sanz, J. L. and Buscalioni, A. D. (1992). A new bird from the Early

Cretaceous of Las Hoyas, Spain and the early radiation of birds. *Paleontol.* **35**, 829–845.

Sanz, J. L., Chiappe, L. M. and Buscalioni, A. D. (1995). The osteology of *Concornis lacustris* (Aves: Enantiornithes) from the Lower Cretaceous of Spain and a reexamination of its phylogenetic relationships. *Am. Mus. Novitates* **3133**, 1–23.

Sanz, J. L., Chiappe, L. M., Perez-Moreno, B. P., Buscalioni, A. D., Moratella, J. J., Ortega, F. and Poyato-Ariza, F. J. (1996). An Early Cretaceous bird from Spain and its implications for the evolution of avian flight. *Nature* **382**, 442–445.

Schufeldt, R. W. (1890). *The Anatomy of the Raven (*Corvus corax sinuatus*).* London: Macmillan.

Simpson, S. F. (1983). The flight mechanism of the pigeon *Columba livia* during take-off. *J. Zool., Lond.* **200**, 435–443.

Sokoloff, A. J., Ryan, J. M., Valerie, D. S., Wilson, D. S. and Goslow, G. E., Jr (1998). Neuromuscular organization of avian flight muscle: morphology and contractile properties of motor units in the pectoralis (pars thoracicus) of pigeon (*Columba livia*). *J. Morph.* **236**, 179–208.

Sonnenblick, E. H. (1962). Force–velocity relations in mammalian heart muscle. *Am. J. Physiol.* **202**, 931–939.

Spiro, D. and Sonnenblick, E. H. (1964). Comparison of the ultrastructural basis of the contractile process in heart and skeletal muscle. *Circulation Res.* **15** (Suppl. 2), 14–36.

Sy, M. (1936). Funktionell-anatomische Untersuchungen am Vogelflugel. *J. Orn.* **84**, 199–296.

Walker, C. A. (1981). New subclass of birds from the Cretaceous of South America. *Nature* **292**, 51–53.

Wang, K., McCarter, R., Wright, J., Beverly, J. and Ramirez-Mitchell, R. (1991). Regulation of skeletal muscle stiffness and elasticity by titin isoforms: A test of the segmental extension model of resting tension. *Proc. Natl. Acad. Sci. USA* **88**, 7101–7105.

Wang, K., McCarter, R., Wright, J., Beverly, J. and Ramirez-Mitchell, R. (1993). Viscoelasticity of the sarcomere matrix of skeletal muscles. *Biophys. J.* **64**, 1161–1177.

Wellenhoffer, P. (1994). New data on the origin and early evolution of birds. *C.R. Acad. Sci. Paris* **319**, 299–308.

Zhou, Z. (1995). New understanding of the evolution of the limb and girdle elements in early birds – evidence from the Chinese fossils. In *Sixth Symposium on Mesozoic Ecosystems and Biota* (ed. Sun, A. and Wang, Y.), pp. 209–214. China Ocean, Beijing.